

Surface water balance at the Chapingo River basin: rainfall intercepted by vegetation and water infiltration into the soil

Pascual-Ramírez, Fermín¹; Prado-Hernández, Jorge V.^{2*}; Martínez-Ruiz, Antonio³; Cristóbal-Acevedo, David²

¹ Universidad Nacional Autónoma de México, Instituto de Investigaciones en Ecosistemas y Sustentabilidad, Antigua Carretera a Pátzcuaro #8701, Col. Exhacienda de San José de la Huerta, Morelia, Michoacán, C.P. 58190.

² Universidad Autónoma Chapingo, Departamento de Suelos, Carretera México-Texcoco km 38.5, Chapingo, Texcoco, México, C.P. 56230.

³ Instituto Nacional de Investigaciones Forestales, Agrícolas y Pecuarias, Campo Experimental Valles Centrales de Oaxaca, C.P. 68200.

* Correspondence: vpradohdez@gmail.com

ABSTRACT

Objective: To estimate the surface water balance in the Chapingo River microbasin in the years 2014, 2016, 2017, and 2018, based on information collected on rainfall and runoff, the use of interception simulation models, and the estimation of the of infiltration as a remainder of the balance.

Design/Methodology/Approach: During the 2014, 2016, 2017, and 2018 wet seasons, the water balance in unit sheet was estimated based on rainfall and runoff data, mathematical interception simulation models, and estimation of infiltration as a remainder of the balance.

Results: The highest interception rate was recorded in 2014, with a shorter range and lower dispersion of rainfall, while the lowest interception occurred in 2018 with opposite rainfall characteristics. A linear relationship was found, in two years, between rainfall and surface runoff with R^2 greater than 0.81. The interception rate was lower in the oyamel fir forest (7.7-9.3%), while the variation in interception between grasslands, pine forests, oak forests, and agricultural areas ranged from 20% to 23%. The remaining infiltration water represented between 85.5% and 88.2% of the rainfall.

Study Limitations/Implications: Determining the temporal evolution of the interception and humidity in the soil is necessary to specify the potential recharge to the aquifer.

Findings/Conclusions: Interception is the main vehicle by which water reaches the ground in areas covered by vegetation. Rainfall intensity has a negative impact on interception and infiltration. The basin under study offers a high recharge potential to the Texcoco aquifer.

Keywords: Hydrology, land-use, intensity, rainfall characteristics, aquifer.

Citation: Pascual-Ramírez, F., Prado-Hernández, J. V., Martínez-Ruiz, A., & Cristóbal-Acevedo, D. (2023). Surface water balance at the Chapingo River basin: rainfall intercepted by vegetation and water infiltration into the soil. *Agro Productividad*. <https://doi.org/10.32854/agrop.v16i9.2586>

Academic Editors: Jorge Cadena Iniguez and Lucero del Mar Ruiz Posadas

Received: May 23, 2023.

Accepted: August 16, 2023.

Published on-line: November 07, 2023.

Agro Productividad, 16(9). September. 2023. pp: 173-180.

This work is licensed under a Creative Commons Attribution-Non-Commercial 4.0 International license.



INTRODUCTION

The Water Balance (WB) is the evaluation of the water cycle variables (rainfall, evapotranspiration, runoff, infiltration, and interception) and is calculated at different observation scales (Sokolov and Chapman, 1974; Xu and Singh, 1998). Rainfall goes

through two fundamental processes: interception by the canopy and infiltration into the soil. Runoff occurs when rainfall exceeds the retention capacity in these two processes. In basins with abundant vegetation, the joint study of rainfall and evapotranspiration allows the modeling of hydrological operations (Sun *et al.*, 2018). Although evapotranspiration (ET) accounts for approximately 40% of the annual accumulated rainfall in temperate climate basins (Shimizu *et al.*, 2003), it is not linked with other elements and, in the absence of rain, most of the water accounted through this method comes from interception (Savenije, 2004). Therefore, during a rain event, the ET can be omitted and the WB elements can be listed as: rainfall, interception, infiltration, and runoff.

At the beginning of a rain event, vegetation retains most of the water (Gerrits *et al.*, 2007; Savenije, 2004). In small rain events, water is stored in the leaves and afterwards evaporates and returns to the atmosphere. When it exceeds the storage capacity of the canopy, it falls to the ground as drops and flows downwards through the stems (Muzylo *et al.*, 2009; Sadeghi *et al.*, 2015); therefore, the water sheet retained and conducted in these processes depends on the type of plant and the morphology of the canopy (Magliano *et al.*, 2022). Although the interception accounts for 20% to 50% of the total rainfall on average (Gerrits *et al.*, 2007), other processes are generally used for its estimation, given the lack of data and the complexity of this process. The interception rate is different between ecosystem components: in temperate forests, it varies from 18% to 60% of the total rainfall (Bolaños-Sánchez *et al.*, 2021; Chen *et al.*, 2013; Flores *et al.*, 2016), in grasslands it approaches 50% and even reaches 100%, depending on the intensity of the rain (Dyer *et al.*, 2022; Ochoa-Sánchez *et al.*, 2018), and in agricultural covers (specifically, corn) its value ranges from 12% to 45% of the total rainfall (Liu *et al.*, 2015; Ma *et al.*, 2016; Zheng *et al.*, 2018).

Both rainfall and runoff (which can be obtained more easily) and, to a lesser extent, interception and infiltration are variables that can be measured to establish explanatory relationships. The simplest approach to WB is to calculate runoff as a fraction of rainfall (Machado *et al.*, 2022). To improve the accuracy of the mathematical models, land cover and use variables are used, along with simplifications of the hydrodynamic characteristics of the soil. The use of these variables results in simple models, such as the curve number (NRCS, 2004), although they do not consider the effect of the interception.

Rain events consists of an initial phase where interception predominates, followed by runoff, which occurs out of phase in time but can be integrated on a daily basis. Therefore, the objective of this research was to estimate the surface water balance in the Chapingo River microbasin in the years 2014, 2016, 2017, and 2018, based on information collected on rainfall and runoff, the use of mathematical simulation models of canopy interception, and estimation of infiltration as a remainder of the balance.

MATERIALS AND METHODS

The Chapingo River microbasin is located in Texcoco, State of Mexico. Its limits are located at 525,057 E, 512,018 W, 2,155,257 N, and 2,147,639 S (UTM 14 N). It has a total area of 1,725.78 ha. The Series VI land-use and vegetation chart was used at a scale of 1:250,000 (INEGI, 2017). The said chart groups five representative sets by dominant vegetation type: rainfed agriculture (18%), pine (*Pinus hartwegii*) forest (25%), oak (*Quercus*

laurina) forest (17%), oyamel fir (*Abies divino*) forest (7%), grassland (13%), and other coverage (20%). The last type includes human settlement polygons, mines, and water bodies.

In the wet season, rainfall records were obtained from two meteorological stations, located in the upper part (Davis[®] station) and the middle part (Hobo[®] station) of the study area. The information was integrated on a daily basis, determining the rainfall every 24 hours, grouped by year of observation.

Surface runoff was recorded at four gauging stations located in the main bed: one in the outlet, another in the lower part, and two more in the middle of the basin. The data were used at the same temporal resolution as rainfall.

Canopy rainfall interception models were used to calculate the interception fraction (%). In the formulations, the intercept (I) is expressed as a percentage (%) and the precipitation (P) in millimeters (mm).

The Zheng *et al.* model was used for agricultural coverage (2018):

$$I = 96.642P^{-0.733} \quad (1)$$

The model of the rainfall-interception ratio in a temperate pine forest —obtained under similar conditions by Bolaños-Sánchez *et al.* (2021)— was adapted to express the intercepted values as a fraction of the rainfall:

$$I = 32.065e^{-0.066P} \quad (2)$$

On the surface covered by oak trees, the model developed by Flores *et al.*, (2016) in the same microbasin was used:

$$I = -6.1571 \ln P + 31.83 \quad (3)$$

The interception simulation on the surface covered by oyamel firs was carried out based on an adaptation of the model developed by Bolaños-Sánchez *et al.* (2021) in the same biome:

$$I = 58.765e^{-0.094P} \quad (4)$$

The grassland interception was obtained with the annual grass model (Corbett and Crouse, 1968):

$$I = (P + 58.7375) / 31.25 \quad (5)$$

The results of the modeling of the interception fraction were converted to a unit sheet (intercepted per event) to integrate the water balance into the temporal resolution of the analysis period.

The infiltration was estimated simplifying the continuity equation:

$$Inf = P - I - SR \quad (6)$$

Where: *Inf* is the infiltration (mm); *P* is rainfall (mm); *I* is the interception (mm); and *SR* is the surface runoff.

The components of the 24-hour water balance were integrated annually for their analysis. Information was used from some rainfall events during which surface runoff had been recorded in four years: 8 in 2014 (August-October), 15 in 2016 (May-August), 8 in 2017 (May-August), and 12 in 2018 (August), with a daily rainfall of 0.8-20.6 mm, 1.1-34.6 mm, 6.9-36.9 mm, and 0.5-45.2 mm, respectively.

RESULTS AND DISCUSSION

The rainfall events analyzed are representative of the rainfall regime of the study site; as shown in Figure 1, there was variability in daily precipitation, with sheets close to unity and extreme sheets similar to those reported by the SMN (2023). The average precipitated sheets of the 2014, 2016, 2017, and 2018 events were 11.5 mm, 14.1 mm, 16.5 mm, and 14.6 mm, respectively, while the standard deviations were 6.8 mm, 9.7 mm, 9.6 mm, and 13.6 mm for the same events.

The resulting water balance showed variations in the distribution of rainfall among infiltration, surface runoff, and canopy retention (Table 1). The rainfall interception fraction had variations of 9% to 12% in the four years, obtaining the highest value in 2014. Although the highest average rainfall in 24 h was recorded in 2017, the lowest interception rate (9.3%) was reported in 2018, as a consequence of the high dispersion of the rain events. Four events were above the 50% average and one reached 200%. Under these conditions, the rain saturated the retention capacity of the canopy and water was directly transferred to the soil surface.

The relative partitioning of rainfall was lower when rainfall intensity increased. These results are similar to the findings of Gerrits *et al.* (2007), given that the interception capacity of the vegetation remains constant. When there are high levels of rainfall in 24 h, the

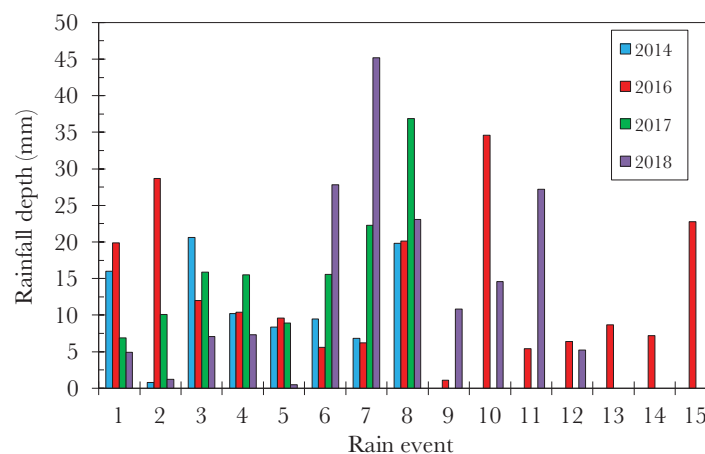


Figure 1. Studied rain events (mm).

Table 1. Elements of the water balance with percentage partitions of rainfall.

Component	2014		2016		2017		2018	
	(mm)	(%)	(mm)	(%)	(mm)	(%)	(mm)	(%)
Rainfall	92.0		198.7		132.1		174.9	
Infiltration	78.7	85.5	175.2	88.2	115.6	87.5	153.7	87.9
Surface runoff	2.0	2.2	2.0	1.0	3.7	2.8	5.2	3.0
Canopy Interception	11.3	12.3	21.6	10.9	12.8	9.7	16.3	9.3

canopy quickly reaches storage saturation and the interception ratio decreases. From that moment onwards, the water that enters the system is distributed only between low-density infiltration and runoff. In vegetation areas, if the intensity of rainfall exceeds the soil infiltration rate, water is lost through runoff. Under these conditions, infiltration depends on the canopy's capacity to transmit water to the soil surface; therefore, infiltration is dependent on interception. Infiltration only occurs at low rainfall rates when the soil is devoid of vegetation; meanwhile, when the intensity exceeds the infiltration capacity of the soil, runoff occurs regardless of the wetting of the soil profile. Shrubs and species with rough bark have a higher interception rate than trees and species with smooth bark (Magliano *et al.*, 2022). Therefore, the interception rate variation depends on the structure and composition of the land cover and use.

The relationship between rainfall and surface runoff had a decoupled behavior: the fraction of instantaneous runoff varied from 1% (2016) to 3% (2018). The differential behavior between rainfall and runoff can be taken as an indication of the spatial distribution of rainfall events. The rainfall and runoff data were analyzed with the linear regression method, finding in all cases a positive slope. However, the adjustment was low, since the R^2 for 2014, 2016, and 2018 was 0.21, 0.49, and 0.10, respectively. Meanwhile, the coefficient of determination for 2017 was high (0.92), mainly because the rains were of low intensity — apart from one event that was 100% higher than the average. In 2018, the extreme rainfall events of August 10 (27.8 mm) and August 11 (45.2 mm) produced low runoff rates; when they were omitted from the rainfall-runoff analysis, the correlation of these two variables reached an R^2 of 0.81. This behavior is a result of the spatial distribution of rainfall, since the information recorded by the two meteorological stations located inside the basin (upper part and middle part) probably did not represent the homogeneous spatial behavior of rainfall expected for a small basin.

Infiltration was estimated as a remnant of the effects of interception and surface runoff, recording an 85.5-88.2% average. Since the mathematical interception models used herein have high proportional values regarding small rain events, when the rainfall sheet is greater than 20 mm, interception does no longer condition the balance and gives way to the infiltration. However, if the intensity per rain event is very high, most of the water is distributed by runoff from the initial stages of the event.

The pine forest (Figure 2) was the cover with the highest interception percentage (22.0-25.5%); these results are similar to the values reported by Bolaños-Sánchez *et al.* (2021) for a *Pinus hartwegii* forest (23.4%). Secondly, rainfed agriculture had values between 22.9%

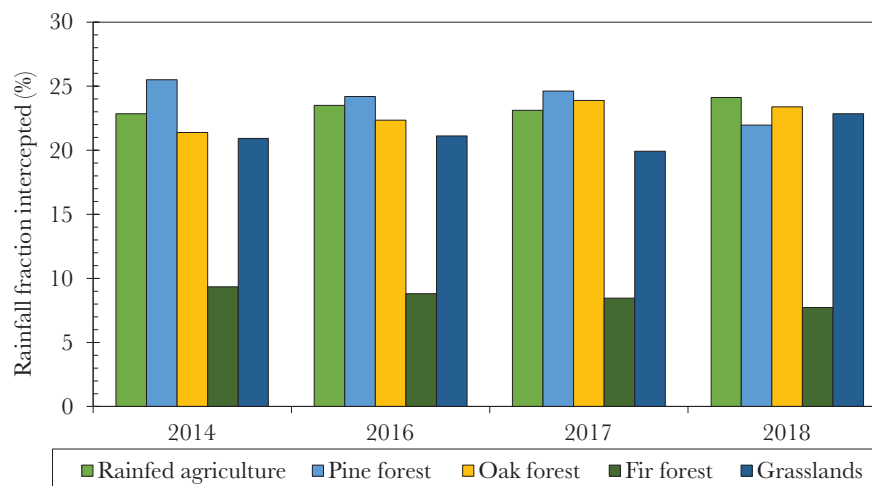


Figure 2. Fraction of rain interception by type of coverage.

and 24.1%, which contrasted with the findings of Zheng *et al.* (2018), who recorded 12.5% in corn crops, with an intensity of 23.1 mm per rain event and high dispersion of rainfall sheets, which ranged from 1.9 mm to 87.8 mm per event. In third place was the oak forest with percentages ranging from 21.4% to 23.4%, which match the 21.7% reported by Flores *et al.* (2016) for an oak (*Quercus laurina*) forest. The grassland had interception percentages ranging from 19.9% to 22.8%, higher than the 12.6% annual value reported for grasslands (Corbett, 1968). The high interception values are the result of the structure and high density of leaves (Corbett & Crouse, 1968; Ochoa-Sánchez *et al.*, 2018). Finally, the oyamel fir forest was the land-use with the lowest interception percentage, with values (7.7-9.3%) below the 37.6% reported in a forest of the same kind in Mexico (Bolaños-Sánchez *et al.*, 2021). These results pertain only to rain events within the wet season; atypical rains outside this period have a different behavior, as a consequence of the variation in the composition of the canopy, especially in deciduous ecosystems. However, the models described in this study lack information for seasonal modeling.

The infiltration values were proportionally high and contributed to filling the storage capacity of the soils. However, in an annual water balance, evapotranspiration becomes a highly relevant element, particularly when the type of coverage is taken into consideration. Mature forests reach high evapotranspiration rates, mainly in the absence of rain events and in the dry season (Nicholls and Carey, 2021). Therefore, most of the water stored by ecosystems in the basins during rain events is consumed by vegetation, leaving a small portion for the recharge of deep aquifers.

The pine forest, oak forest, rainfed agriculture, and grassland land-uses had a similar interception percentage, with an approximately 5% variation between their values.

The differences between the results of this research and those reported in other studies are attributed to the effect of climatological variations (Herwitz A' and Slye, 1995; Ochoa-Sánchez *et al.*, 2018), since factors such as the duration of rainfall events and the intensity, and spatial pattern of rainfall, as well as the circulation of air masses and the seasons of the

year, impact the interception values. For example, convective rains impact smaller areas than orographic rains which, in turn, are smaller than frontal or cyclonic rains.

The best adjustments to the modeling of the rainfall-interception ratio occur when rainfall events are analyzed on an individual basis, rather than when they are grouped over time (Bolaños-Sánchez *et al.*, 2021). The change in land-use from forest to cropland causes the infiltration rate to decrease by up to 58% (Sun *et al.*, 2018); This proportion of water that cannot be infiltrated is added to the runoff fraction. If the infiltration rate decreases in a basin, the recharge rate of the underground aquifers decreases and, consequently, the base flow of the drainage network also decreases.

CONCLUSIONS

The WB analysis determined that rainfall is mainly divided into interception—in the case of small events—and infiltration—when the canopy and its water storage capacity are saturated. Runoff occurs as a result of high intensity or saturation of the interception. Interception in the four years ranged from 9% to 12% of the rainfall. However, most of the water transmitted to the soil was first intercepted, therefore the interception influences in the effect of water into the soil. The oyamel fir forest had the lowest interception rate, while the rest of the coverages analyzed had variations of 5% between each other. The study basin is a source of the Texcoco aquifer with great recharge potential, owing to an average annual soil infiltration of 87.3% of rainfall.

REFERENCES

- Bolaños-Sánchez, C., Prado-Hernández, J. V., Silván-Cárdenas, J. L., Vázquez-Peña, M. A., Madrigal-Gómez, J. M., & Martínez-Ruiz, A. (2021). Estimating rainfall interception of *Pinus hartwegii* and *Abies religiosa* using analytical models and point cloud. *Forests*, *12*(7). <https://doi.org/10.3390/f12070866>
- Chen, S., Chen, C., Zou, C. B., Stebler, E., Zhang, S., Hou, L., & Wang, D. (2013). Application of Gash analytical model and parameterized Fan model to estimate canopy interception of a Chinese red pine forest. *Journal of Forest Research*, *18*(4), 335–344. <https://doi.org/10.1007/s10310-012-0364-z>
- Corbett, E. S., & Crouse, R. P. (1968). Rainfall interception by annual grass and chaparral . . . losses compared. Res. Paper PSW-RP-48, Forest Service, U.S.D.A.
- Dyer, D. W., Patrignani, A., & Bremer, D. (2022). Measuring turfgrass canopy interception and throughfall using co-located pluviometers. *PLoS ONE*, *17*(9 September). <https://doi.org/10.1371/journal.pone.0271236>
- Flores, E., Guerra, V., Terrazas, G., Carrillo, F., Islas, F., Acosta, M., & Buendía, E. (2016). Intercepción de lluvia en bosques de montaña en la cuenca del río Texcoco, México. *Revista Mexicana de Ciencias Forestales*, *37*(7), 65–76.
- Gerrits, A. M. J., Savenije, H. H. G., Hoffmann, L., & Pfister, L. (2007). Hydrology and Earth System Sciences New technique to measure forest floor interception—an application in a beech forest in Luxembourg. In *Hydrol. Earth Syst. Sci* (Vol. 11). www.hydrol-earth-syst-sci.net/11/695/2007/
- Herwitz A, S. R., & Slye, R. E. (1995). Three-dimensional modeling of canopy tree interception of wind-driven rainfall. In *Journal of Hydrology ELSEVIER Journal of Hydrology* (Vol. 168, Issue 1).
- Instituto Nacional de Estadística y Geografía (INEGI), 2017. Carta de Uso de Suelo y Vegetación Serie VI escala 1:250,000.
- Liu, H., Zhang, R., Zhang, L., Wang, X., Li, Y., & Huang, G. (2015). Stemflow of water on maize and its influencing factors. *Agricultural Water Management*, *158*, 35–41. <https://doi.org/10.1016/j.agwat.2015.04.013>
- Ma, B., Li, C. D., Ma, F., Li, Z. bin, & Wu, F. Q. (2016). Influences of Rainfall Intensity and Leaf Area on Corn Stemflow: Development of a Model. *Clean - Soil, Air, Water*, *44*(8), 922–929. <https://doi.org/10.1002/clen.201500050>
- Machado, R. E., Cardoso, T. O., & Mortene, M. H. (2022). Determination of runoff coefficient (C) in catchments based on analysis of precipitation and flow events. *International Soil and Water Conservation Research*, *10*(2), 208–216. <https://doi.org/10.1016/j.iswcr.2021.09.001>

- Magliano, P. N., Whitworth-Hulse, J. I., Cid, F. D., Leporati, J. L., van Stan, J. T., & Jobbágy, E. G. (2022). Global rainfall partitioning by dryland vegetation: Developing general empirical models. *Journal of Hydrology*, 607. <https://doi.org/10.1016/j.jhydrol.2022.127540>
- Muzyló, A., Llorens, P., Valente, F., Keizer, J. J., Domingo, F., & Gash, J. H. C. (2009). A review of rainfall interception modelling. *Journal of Hydrology*, 370(1–4), 191–206. <https://doi.org/10.1016/j.jhydrol.2009.02.058>
- Nicholls, E. M., & Carey, S. K. (2021). Evapotranspiration and energy partitioning across a forest-shrub vegetation gradient in a subarctic, alpine catchment. *Journal of Hydrology*, 602. <https://doi.org/10.1016/j.jhydrol.2021.126790>
- NRCS. (2004). Chapter 10 Estimation of Direct Runoff from Storm Rainfall.
- Ochoa-Sánchez, A., Crespo, P., & Céleri, R. (2018). Quantification of rainfall interception in the high Andean tussock grasslands. *Ecohydrology*, 11(3). <https://doi.org/10.1002/eco.1946>
- Sadeghi, S. M. M., Attarod, P., & Pypker, T. G. (2015). Differences in Rainfall Interception during the Growing and Non-growing Seasons in a *Fraxinus rotundifolia* Mill. Plantation Located in a Semiarid Climate. In *J. Agr. Sci. Tech* (Vol. 17).
- Savenije, H. H. G. (2004). The importance of interception and why we should delete the term evapotranspiration from our vocabulary. *Hydrological Processes*, 18(8), 1507–1511. <https://doi.org/10.1002/hyp.5563>
- SMN (Servicio Meteorológico Nacional). (2023). Información de precipitación de la normal climatológica de Chapingo. Accedido: 15 de enero 2023, de <https://smn.conagua.gob.mx/es/informacion-climatologica-por-estado?estado=mex>
- Shimizu, A., Shimizu, T., Miyabuchi, Y., & Ogawa, Y. (2003). Evapotranspiration and runoff in a forest watershed, western Japan. *Hydrological Processes*, 17(15), 3125–3139. <https://doi.org/10.1002/hyp.1261>
- Sokolov, A., & Chapman, V. (1974). Methods for water balance computations. An international guide for research and practice. In *The UNESCO Press* (Vol. 23, Issue March). <https://doi.org/10.1017/CBO9781107415324.004>
- Sun, D., Yang, H., Guan, D., Yang, M., Wu, J., Yuan, F., Jin, C., Wang, A., & Zhang, Y. (2018). The effects of land use change on soil infiltration capacity in China: A meta-analysis. *Science of the Total Environment*, 626, 1394–1401. <https://doi.org/10.1016/j.scitotenv.2018.01.104>
- Xu, C., & Singh, V. P. (1998). A Review on Monthly Water Balance Models for Water Resources Investigations. *Water Resources Management*, 12(1), 31–50. <https://doi.org/09204741>
- Zheng, J., Fan, J., Zhang, F., Yan, S., & Xiang, Y. (2018). Rainfall partitioning into throughfall, stemflow and interception loss by maize canopy on the semi-arid Loess Plateau of China. *Agricultural Water Management*, 195, 25–36. <https://doi.org/10.1016/j.agwat.2017.09.013>